THE ASTROPHYSICAL JOURNAL, 347:1119–1127, 1989 December 15

FAR-INFRARED SPECTROPHOTOMETRY OF SN 1987A: DAYS 265 AND 267

S. H. MOSELEY,[1] E. DWEK,[1] W. GLACCUM,[2] J. R. GRAHAM,[3] R. F. LOEWENSTEIN,[4] AND R. F. SILVERBERG[1]

Received 1988 September 12; accepted 1989 June 13

ABSTRACT

We present 16–66 μm spectra of SN 1987A taken on days 266 and 268 after core collapse. The spectrum consists of a nearly flat continuum, strong emission lines of hydrogen, and fine-structure lines of Fe II, Fe III, Co II, S I, and possibly Fe I, Ni II, and S III. From the relative strength of three lines which arise from transitions within the ground and excited states of Fe II, we derive the temperature and a lower limit on the density of the line-emitting region. From the line strengths, we estimate the abundances of Fe and S I, end products of explosive nucleosynthesis in the supernova. We are also able to set an upper limit to the amount of Co II remaining in the mantle. The low measured mass of Fe suggests that the ejecta are clumpy. The flat continuum is most likely free-free emission from the expanding supernova ejecta. About 35% of this emission arises from the ionized metals in the mantle; the rest arises from ionized hydrogen. At the time of these observations, there is no evidence for any emission from dust that may have formed in the supernova ejecta or from preexisting dust in the surrounding medium.

Subject headings: infrared: spectra — line identifications — spectrophotometry — stars: abundances — stars: individual (SN 1987A) — stars: supernovae

I. INTRODUCTION

The extremely rare occurrence of a nearby supernova (SN) provides astronomers with a unique opportunity to conduct a detailed multiwavelength analysis of this event and its effect on the ambient medium. Infrared (IR) observations of SN 1987A can provide information on the chemical composition and kinematics of the ejected material (Meyerott 1980; Axelrod 1980; Fransson and Chevalier 1987; Colgan and Hollenbach 1988), the formation of dust in the outflow (Gehrz and Ney 1987; Dwek 1988*a*; Kozasa, Hasegawa, and Nomoto 1989), the presence of dust around the supernova (Dwek 1988*b*), and the interaction of the supernova blast wave with the surrounding dusty medium (Itoh 1987; Dwek 1988*b*).

The determination of the abundances of the heavy elements synthesized in stellar interiors and explosions is a highly coveted goal in astronomy. Prior to SN 1987A, abundance determinations have been limited to young supernova remnants, whose ejecta have not yet been mixed with the general interstellar medium (ISM), and to select regions of the ejecta, namely fast-moving knots or filaments that have been interacting with the ambient medium (e.g., Chevalier and Kirshner 1979 for Cas A; Winkler and Kirshner 1987 for Pup A). SN 1987A provides astronomers with their first "unbiased" look at the composition of the expanding debris of a supernova. Far-infrared (FIR) observations of the supernova have several distinct advantages over other wavelength regimes in probing the elemental abundances in the ejecta. The FIR portion of the spectrum contains many fine-structure lines of heavy elements such as Co, Fe, S, Si, and O that are synthesized in massive stars and SN explosions. Many of these lines can be detected with high signal-to-noise ratios, and their analysis is relatively uncomplicated by radiative transfer effects and line blending. The fine-structure lines can therefore be used to determine elemental abundances without substantial sensitivity to the adopted physical conditions. For example, the 16–30 μm region contains many fine-structure lines of Fe I, Fe II, and Fe III, which are expected to be the dominant ionization states in the ejecta. We thus expect to get a reliable estimate of the total abundance of iron, one of the most abundant end products of explosive nucleosynthesis. Fine-structure line ratios, such as the forbidden 17.93 and 25.98 μm lines, arising, respectively, from the $J = 7/2 \rightarrow 9/2$ transition in the first electronically excited state and ground state of Fe II, can be used as a temperature diagnostic of the ejecta. Finally, the line velocity profile can provide information about the dynamics of the explosion and the degree of mixing among the various layers of the star.

The presence of isotropic anomalies in meteorites suggests that dust must form in supernova ejecta (e.g., Clayton 1982). Any dust that will form in the ejecta can potentially be identified by its IR emission (Gehrz and Ney 1987; Dwek 1988*a*). Since the dust is expected to form near the condensation temperature, most dust candidates may, depending on the available heating sources, produce an initial spectrum peaking between 3 and 5 μm which would decline more rapidly than a blackbody at longer wavelengths. The subsequent evolution of the IR spectrum would depend on that of the heating sources.

FIR observations of the SN may also be useful in setting constraints on the presence and properties of dust existing in the surrounding medium prior to the SN explosion and may be used to observe the interaction of the supernova blast wave with the ambient dusty medium which will give rise to FIR emission from collisionally heated dust (Itoh 1987; Dwek 1988*b*).

II. THE OBSERVATIONS

a) Instrument Characteristics

On 1987 November 17 and 19, we carried out the first far-infrared spectrophotometric observations ever made of a supernova. The observations were made aboard the Kuiper Airborne Observatory (KAO), flying out of Christchurch, New

[1] Laboratory for Astronomy and Solar Physics, NASA/Goddard Space Flight Center.
[2] Applied Research Corporation.
[3] Downs Laboratory, California Institute of Technology.
[4] Yerkes Observatory, University of Chicago.

Zealand, with the Goddard 24 channel grating spectrophotometer. The instrument is a helium-cooled spectrophotometer which uses an array of 24 ^{3}He-cooled bolometers as detectors. It employs two gratings operated in first order. Observations were made simultaneously over the full spectral range of each grating configuration with one detector per spectral resolution element. The spectral resolution was detector-size limited at 0.6 μm with 16–30 μm grating, and 1.8 μm in the 35–66 μm range. The detectors are composite bolometers using Si : Sb compensated with boron as thermometers, each of which has arsenic ion-implanted contacts and Cr-Au metallization for electrical contact. The substrate for the absorber is Si about 25 μm thick, and the absorbing layer is a Cr Au film deposited to an impedance of $\sim$170 Ω per square which gives nearly flat spectral response over the entire spectral range with 50% quantum efficiency. As operated in November, the instrument was limited by background noise in the 16–30 μm and 35–50 μm ranges. Beyond 50 μm, the instrument was limited by either amplifier or detector noise.

b) *Calibration*

The observations on November 17 were calibrated using Callisto (J4) as the flux standard at all wavelengths. The brightness temperature of Callisto was modeled (Glaccum 1989) with a two-temperature fit similar to Spencer's (1987) fits to the *Voyager* IRIS data. During both flights, November 17 and 19, we also observed VY CMa, a bright source characterized by a smooth spectrum, before, during, and after the SN observations to monitor the instrument stability and to provide a transfer of calibration to the November 19 flight. To test the Callisto model, and to verify the quality of the entire calibration scheme, we compared the fluxes of γ Cru, η Car, and VY CMa, obtained with the Callisto model, to their fluxes as determined by us in 1986 April using Mars as a radiometric standard (Wright 1976; Odenwald 1983). The flux for γ Cru, measured in the 16–30 μm range, was within 1% of the value we measured in 1986 April. To compare the Callisto model to Mars over the 30–66 μm range, we scaled the fluxes of both η Car and VY CMa as measured with respect to the two calibrators to match over the 20–30 μm range, since they are variable and the calibrations were done at different times. Once scaled, their spectra derived from the two calibrations agree to within 10% between 35 and 60 μm. Also, in 1986 April, we verified the Wright model for Mars by calibrating it against Uranus, which is the most accurately calibrated far-infrared point source out to 50 μm. Using a full-disk model by Conrath (1986) derived from the *Voyager* IRIS measurements (Hanel *et al.* 1986), the Wright model agreed with our measured flux of Mars within 3% at 33 μm and 2% at 50 μm. We therefore believe our observed fluxes to be absolutely accurate to better than $\sim$10% between 20–30 μm, and better than 15% at the longer wavelengths.

The spectral response of each channel was measured prior to the KAO flights with 0.25 cm^{-1} spectral resolution using a Fourier transform spectrometer. This high resolution is required to accurately determine the transmission of the instrument/atmosphere combination, since the H_2O and CO_2 lines in the atmosphere are quite narrow at high altitudes and the interference fringes in the filters can be comparably narrow. In the data reduction process, atmospheric H_2O values are determined on "smooth spectrum" objects by choosing the value which produces the smoothest spectrum near the H_2O lines. Such objects were observed before, at intervals during, and after the SN observations. Conditions were uniformly good during these observations, and no large changes in H_2O were seen. Since the onboard water vapor radiometer tracked the derived H_2O column density well, the values from it were used for the true H_2O column density during the SN observations. While some uncertainties arise from imperfect corrections for atmospheric H_2O absorption (Glaccum 1989), these errors are much smaller than the statistical errors for these supernova observations.

b) *Observational Results*

The data presented in this paper are the result of 2 hr of integration in the short-wavelength configuration and 1.5 hr in the long-wavelength configuration of our instrument. The observations were taken on the two nights are of similar quality, and are, within statistical errors, in agreement with each other. Figure 1 depicts the 16–30 μm and 35–66 μm spectra of SN 1987A. The short-wavelength spectrum is characterized by strong emission lines, which account for about 20% of the flux in this wavelength region. A continuum at a level of about 8–10 Jy dominates the emission at the longer wavelengths, with evidence for excess emission at the wavelength of strong H recombination lines. At wavelengths longer than 30 μm, the continuum is not as smooth, with some evidence of lower flux in the 40–45 μm region, or excess emission near 60 μm compared to the flat 10 Jy continuum seen in the 16–30 μm range. To derive the flux densities, we assumed initially that the supernova spectrum is flat over the width of each channel. The mean flux density is then equal to the total power measured in each spectral channel divided by its effective bandwidth. As discussed in more detail later on, line intensities were derived by creating a synthetic spectrum which was subsequently convolved with the spectral response of each channel (see Fig. 2). The strength of the line and continuum components were then adjusted to produce the observed power in the various channels. In the following section, we discuss the identification of the lines in the spectrum and derive their strengths. The continuum emission is treated in § IV.

III. THE LINE-EMISSION COMPONENT

a) *Line Identifications*

We have strong theoretical prejudices about which lines should be strong in the far-infrared spectrum. Before the observations were made, we calculated the ionization state following Meyerott (1980) and Axelrod (1980) in the ejecta of Woosley, Pinto, and Ensman's (1987) 15 $M_\odot$ supernova model to demonstrate the feasibility of the proposed observations. The brightest lines in the wavelength region of interest were due to O, Si, S, and the iron group. The ionization level of the ejecta was found to be low, with lines of neutral, singly, and doubly ionized species dominating the spectrum. The same conclusion was reached by Fransson and Chevalier (1987). Despite this bias, we have compiled a list of all potential candidate lines with wavelengths that coincided with all the features in our spectrum (except the broad long-wavelength continuum structure mentioned above) that have a level greater than 4 σ above the continuum. For elements up to Ca, we used a line list from Wiese, Smith, and Glennon (1966) and Wiese, Smith, and Miles (1969), supplemented and updated where necessary by Mendoza's (1983) atomic data compilation. A list of the lines from iron group elements was compiled from various sources in the literature. The resulting line candidates are listed in Table 1.

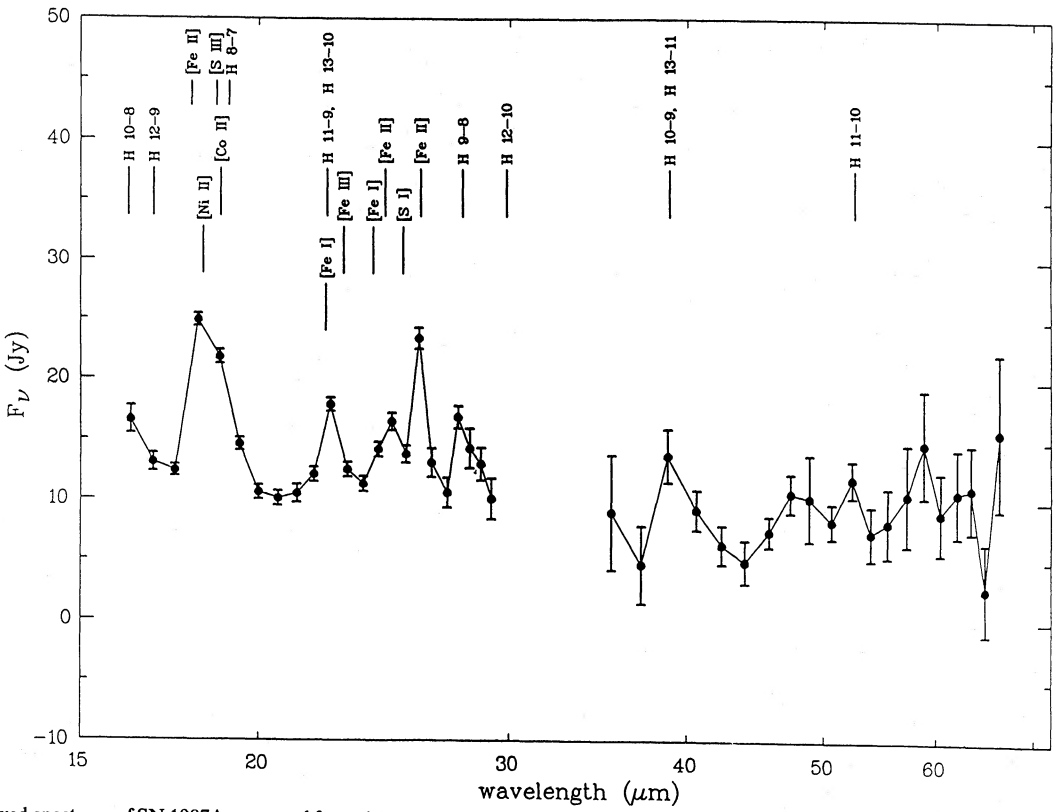

FIG. 1.—Observed spectrum of SN 1987A, averaged from days 266 and 268. Flux densities for each channel are computed by assuming the supernova spectrum to be flat (S_ν = constant) over the channel. Passbands are trapezoidal with steep edges.

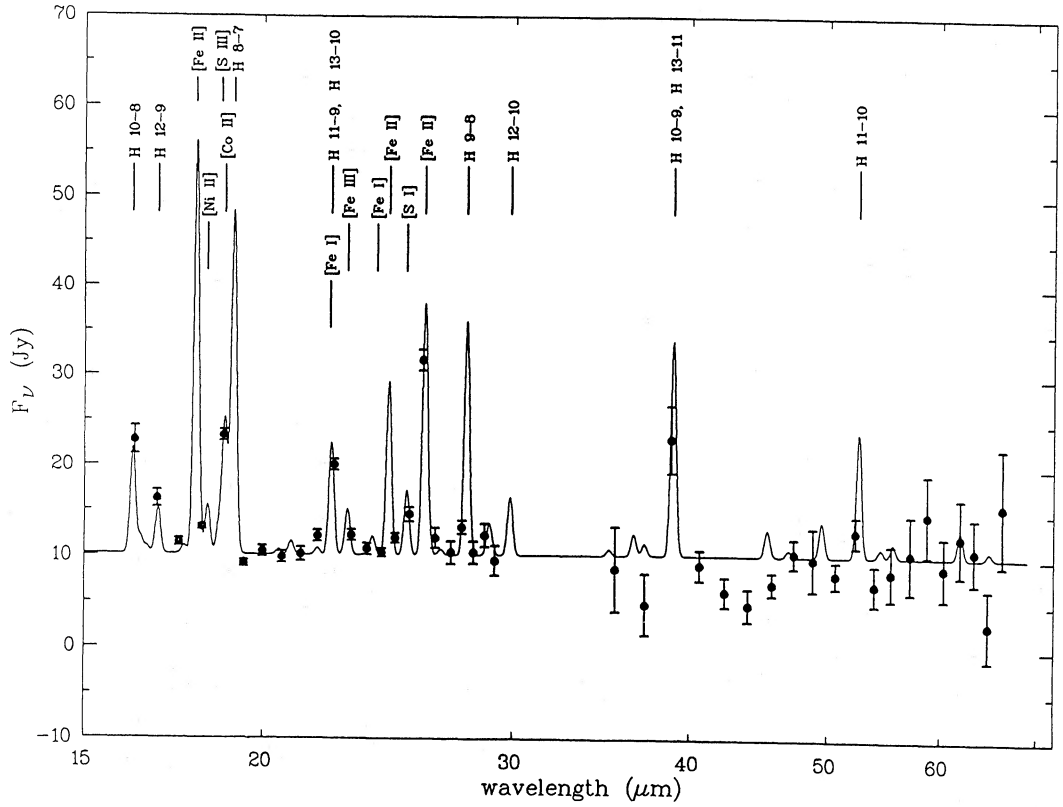

FIG. 2.—Color-corrected monochromatic flux densities for SN 1987A and the synthetic spectrum. Synthetic spectrum and monochromatic flux densities at bandpass centers are derived iteratively from the data in Fig. 1, as described in the text. In this representation, a perfect fit would be achieved when all the data points lie on the synthetic spectrum. The unlabeled weak lines are H recombination lines. For $\lambda > 30$ μm, lines of elements other than H are not included in the synthetic spectrum. If H8-7 has a symmetric line shape, it contributes equal amounts to the two adjacent channels.

TABLE 1

LINE IDENTIFICATION ON THE BASIS OF WAVELENGTH COINCIDENCES

Channel Number	λ_0 (μm)	Identification
27	16.27	H I 8–10 16.21, Co III 16.38
26	16.87	H I 9–12 16.88
24	18.14	Fe II 17.93, Ca VI 17.98, Cl VI 18.08 Ni II 18.24, S IV 18.28
23	18.78	Co II 18.80, S III 18.68, H I 7–8 19.06
22	19.39	H I 7–8 19.06
17	22.46	H I 9–11 22.34, H I 10–13 22.33, Fe I 22.29
12	23.09	Fe III 22.92
10	24.26	Fe I 24.04, Fe II 24.52
9	24.80	F I, 24.75, Fe II 24.52
8	25.38	S I 25.25, Co II 25.67
7	25.93	Fe II 25.98, F IV 25.75, O IV 25.87, Co II 25.67
4	27.62	H I 8–9 27.80

TABLE 2

LINE FLUXES

Species	Flux (10^{-11} ergs s^{-1} cm^{-2})
[Fe II] 17.93 μm	8.2 ± 0.4
[Co II] 18.80 μm + [S III] 18.68 μm	2.4 ± 0.3
H I 8-7 19.06	6.2 ± 0.5
[Fe III] 22.9 μm	0.7 ± 0.2
[Fe II] 24.52 μm	2.5 ± 0.3
[S I] 25.25 μm	0.6 ± 0.2[a]
[Fe II] 25.98 μm	3.4 ± 0.2
H I 9-8 27.80	3.0 ± 0.3

[a] The strength of the S I line has been reduced by 40% from the value derived from the synthetic model fittings to allow for the contribution of Co II emission at 25.67 μm which was not included in the synthetic model. The strength of the 25.67 μm Co II line was scaled from the derived strength of the 18.80 μm Co II line.

Our theoretical calculations, and the absence of lines arising from high-ionization states at optical wavelengths (Phillips *et al.* 1988) suggest that species with high ionization potentials, such as Ca VI (I_{ion} = 108.8 eV) and O IV (I_{ion} = 77.4 eV), are not likely candidates. We can also exclude F I on the basis of its low expected abundance. Co III is not a likely candidate either, since [Co III] 11.89 μm was not observed in the shorter wavelength observations of Rank *et al.* (1988). We are therefore left with only H, S, Fe, Co, and Ni as potential line sources.

b) *Line Strength Determination*

Having identified line candidates for the 16–30 μm spectral range, we must estimate the line strengths required to produce the observed signal through the measured instrumental passbands and calculated atmospheric transmission. We first subtracted the continuum emission component, which was assumed to be flat and featureless and was found to have a value of 10.2 Jy over this spectral range. A single scale factor for the H line-emission strength was adjusted, with the relative strength of the lines being set according to the model of Brockelhurst (1970, 1971) for $n_e = 10^6$ cm^{-3} and $T = 7500$ K. All H lines falling in this spectral range with upper level indices of 20 or less were included in the calculations.

To fit the spectrum, we assumed that all line shapes were Gaussian with 3000 km s^{-1} FWHMs. The scale factor for the H lines was then adjusted so that the data fit the unblended lines (see Fig. 2) H10-8, H12-9, H11-9, and H9-8, and the unblended portion of H8-7 which illuminated channel 22. In the resulting synthetic spectrum, H10-8, H12-9, and H9-8 are slightly too weak compared to the observations, while H8-7 is slightly too strong.

Having adopted continuum and H line strengths, we can now adjust the strength of the lines of Fe, Co, and S to produce the best fit to the observed spectrum. The lines were assumed to be 3000 km s^{-1} FWHM Gaussians, but our results are not sensitive to variations of up to a factor of 2 in assumed line width. The errors in line strength represent the change in assumed line strength which results in a 1 σ deviation from the measured flux in the relevant channel. The line fluxes and errors are given in Table 2.

c) *The Size of the Emitting Region*

Since the line widths are significantly narrower than our instrumental resolution, we cannot measure the expansion velocity to determine the radius of the line-emitting region. However, we can obtain a lower limit on the radius, R, of the line-emitting region by calculating the radius of a blackbody that will give rise to the same intensity as observed in the line. For $R = vt$, and a line width of Δv given by $\Delta v = v(v/c)$, the radius is given by

$$R = [cLt/4\pi^2 v B_\nu(T)]^{1/3} , \quad (1)$$

where v is the velocity of the emitting surface, L is the luminosity in the line, t is the time since the expansion began, T is the gas temperature taken to be 6000 K, and homologous expansion with a velocity $v = r/t$ has been assumed, where r is the distance from the center of the explosion. From the emission in channel 7 at 25.9 μm, which corresponds to the unblended Fe II ground-state transition, we derive $R = 4.0 \times 10^{15}$ cm (corresponding to $v = 1700$ km s^{-1} and the derived temperature of 6000 K). In § IV we derive a similar lower limit on the size of the free-free emitting region. Since most of the energy output from the radioactive decay of ^{56}Co (the progenitor of ^{56}Fe) is converted to optical radiation, the size of the optical line-emitting region should also be comparable to that of the IR line-emitting region at the time of our observations.

d) *The Temperature in the Line-emitting Region*

In the following, we will estimate the temperature in the emitting region from the various temperature-sensitive line ratios. The assumption in these calculations is that the lines are optically thin. In § III*e* below, we show that some of the lines may be optically thick, and we discuss the implication of this result on the derived temperatures. The energy, in the form of gamma rays from the radioactive decay of ^{56}Co, is rapidly thermalized in the surrounding medium, heating the thermal electron gas. The population of the low-lying levels ($E < 2000$ cm^{-1}; $T < 2800$ K) of ions such as Fe II is determined by the balance of collisional excitation by these thermal electrons and spontaneous radiative decay (Meyerott 1980; Axelrod 1980). Therefore, line ratios that compare the strength of a ground-state transition to that from an excited state are sensitive to electron temperature and can be used as temperature diagnostics of the ejecta. There are three such line ratios, [Ni II] (18.24)/[Ni II] (6.64), [Fe II] (25.98)/[Fe II] (17.94), and [Fe II] (24.5)/[Fe II] (25.98), that are sensitive to the electron temperature and density. The 18.24 μm [Ni II] line comes from an excited state with upper level at 10,663 cm^{-1} ($T \approx 15{,}300$ K), and the 17.94 and 24.5 μm transitions in Fe II arise, respec-

tively, from the 2430 cm^{-1} ($T = 3500$ K) and 2837 cm^{-1} ($T = 4087$ K) excited states in Fe II. The problem is that the three line ratios cannot be determined independently, since the 17.94 μm Fe II flux is blended with the 18.24 μm Ni II line in channel 24 (see Table 2). The contribution of the [Ni II] 18.24 μm line can, however, be estimated from the strength of the [Ni II] 6.64 μm line, identified in the spectra of Rank *et al.* (1988). Assuming high electron densities and using the atomic data of Nussbaumer and Storey (1982), we get that the contribution of the Ni II line will reduce the flux of the 17.94 μm [Fe II] line by 16% at 7000 K, and by 27% at 10,000 K. To calculate the ionic abundances and electron temperatures in a self-consistent manner, we adopted the iterative procedure described below. We first calculated the level population of Fe II and the various line ratios described above for a grid of electron densities and temperatures. Details of the models are described in Graham *et al.* (1986) and Graham, Wright, and Longmore (1987). Current models were updated to include recent eight configuration calculation of Fe II Einstein *A*-values by Nussbaumer and Storey (1988*a*). Figure 3 depicts the contours of the [Fe II] (25.98)/[Fe II] (17.93) line ratio on the (n_e, T) plane. For the observed ratio of 0.41 $\pm$ 0.04, the inferred electron temperature is 6000^{+2000}_{-1000} K at high densities. The figure shows that at densities in the range inferred from the free-free emission; i.e., for $n_e > 10^7$ cm^{-3}, the line ratios are just given by a Boltzmann level population and are independent of electron density. The same behavior holds true for the [Fe II] (24.5)/[Fe II] (25.98) ratio we considered. The temperature derived from the observed [Fe II] (24.5)/[Fe II] (25.98) line ratio is 5100^{+1900}_{-1300} K. At this range of temperatures the [Ni II] 18.2 μm transition contributes significantly to the channel 24 flux. Temperatures derived from the [Fe II] (25.98)/[Fe II] (17.93) flux ratio which do not account for the Ni II line contribution will therefore be systematically too high. The temperature that yields the best fit to the three flux ratios can therefore only be obtained by an iterative procedure in temperature, in which the [Fe II] 17.94 flux is corrected at each step for the contribution of the [Ni II] 18.2 μm flux at that temperature. For example, in the first iteration we derive a temperature of 5100 K from the [Fe II] (24.5)/[Fe II] (26.0) flux ratio. Subtracting the [Ni II] 18.2 μm contribution to the [Fe II] 17.9 flux then yields a [Fe II] (26.0)/[Fe II] (17.9) derived temperature of 7000^{+2400}_{-1400} K, which agrees with the initially determined temperature at the 1 σ level. Further iterations improve the fit, and we find that the best agreement between the temperature diagnostics is obtained when $T = 6000^{+2000}_{-1000}$ K. The electron density is only weakly constrained by the [Fe II] line ratios to be greater than 10^4 cm^{-3}.

e) Abundances

The emissivity of ground-state fine-structure transitions depends, for $h\nu \ll kT$ and thermal equilibrium, only on the level partition function and the Einstein *A*-coefficients for the transition. Therefore, the mass of emitting species which are represented by such transitions (Fe I, Fe II, Fe III, S I, and S III) can be derived essentially without knowledge of the temperature. However, the Co II line comes from an excited state at 4560 cm^{-1} ($T_{ex} = 6560$ K), and therefore the mass of Co II depends on the temperature. In Table 3, we list the masses of the detected species for $T = 6000^{+2000}_{-1000}$ K. An *A*-value of 0.011 s^{-1} was adopted for the [Co II] $J = 4 \rightarrow 3$ transition in the $a\,^5F$ multiplet at 18.80 μm (Nussbaumer and Storey 1988*b*). The large errors in the Ni II and Co II masses are due to the temperature sensitivity of the emissivity of these excited state lines. It should be noted that these masses must be thought of as lower limits, because the lines may be optically thick. The

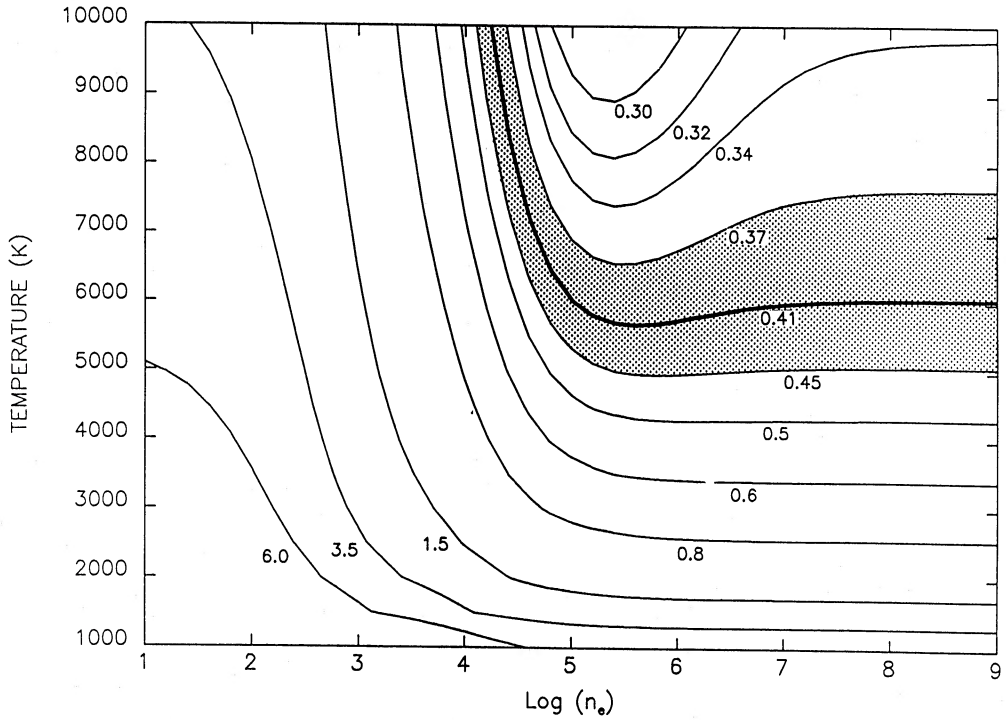

FIG. 3.—Contours of the [Fe II] (25.98)/[Fe II] (17.93) line ratio are plotted on the (n_e, T)-plane. Heavy contour is drawn at the observed ratio of 0.41, and the area within 1 σ ($\sigma = 0.04$) is shaded. For the observed ratio of 0.41, the inferred electron temperature is 6000 K. At densities in the range inferred from the free-free emission, i.e., for $n_e > 10^7$ cm^{-3}, line ratios are just given by a Boltzmann level population and are independent of electron density.

entries in the table for S III and Co II are calculated assuming that each ion is the sole contributor to the observed flux in the channel (after the contribution from the H lines has been subtracted). Their tabulated masses should therefore be considered as strict upper limits, unless they are optically thick. Considering the low ionization state of the ejecta, we believe Co II to be the dominant contributor to the excess flux in the channel.

Table 2 shows that the ionization state of the ejecta is low and that Fe II is the dominant ionization stage of Fe. It is therefore unlikely that a large fraction of Fe is present as Fe IV. The mass of iron is therefore well represented by the sum of the masses of the three observed ionization stages, i.e., $M(\mathrm{Fe}) = M(\mathrm{Fe\ I}) + M(\mathrm{Fe\ II}) + M(\mathrm{Fe\ III}) = 0.021 \pm 0.0015\ M_\odot$. This error reflects only the uncertainty in the determination of line strengths. The total error in mass is dominated by the uncertainty of the A-value for the transition. This error cannot be as large as 40% and is likely to be much less than 30%, which corresponds to a mass uncertainty of $0.006\ M_\odot$. We know from the bolometric light curve that $0.075\ M_\odot$ of radioactive ^{56}Ni was synthesized in the explosion (Woosley 1988; Itoh *et al.* 1987), of which $0.068\ M_\odot$ will have decayed to stable ^{56}Fe by the time of these observations. We therefore observe only about one-third of the Fe which should be in the ejecta. It is important to understand why we do not see all of the Fe. The missing Fe could be either too hot or too cold to emit strongly. At sufficiently low temperatures ($T \ll 1000$ K), the fine-structure transitions are not excited, and at high temperature ($T \gg 10{,}000$ K), the partition function becomes large and the population in the ground state is reduced. These temperatures are too extreme for this to be a plausible solution. It is much more likely that the strong [Fe II] lines are optically thick. If so, then not only the abundances, but the temperature previously derived from the line ratios, may be in error. The lines that become optically thick first are the lower lying energy transitions. At finite optical depths, the [Fe II] 26.0/[Fe II] 24.5 and [Fe II] 26.0/[Fe II] 17.9 line ratios will be higher than implied from the observations, and the derived temperature will then overestimate the actual temperature in the ejecta.

TABLE 3

DERIVED MASSES IN THE EJECTA

Ion	Mass ($M_\odot$)
Fe I	< 0.003 (3 σ)
Fe II	0.019 ± 0.001
Fe III	0.0015 ± 0.0004
Ni II	0.0038 ± 0.0014
Co II[a]	0.0043 ± 0.0014
S III[a]	0.0016 ± 0.002
S I[b]	0.0013 ± 0.0008

[a] Mass quoted assumes that all the flux detected at 18.7 μm, after the subtraction of the H7-8 contributions, is due to only that species, and that the ejecta is optically thin in the line. The masses for Co II and S III may therefore be thought of as upper limits.

[b] Actual mass of S I has been reduced by 40% from the value derived from the synthetic model to correct for contribution of the Co II line at 25.67 μm which was not included in the model (see Table 2).

We estimate first the optical depth from the probability, P, that a photon escapes without further interaction. In the escape probability approximation, P is given by

$$P = 1/\tau[1 - \exp(-\tau)], \quad (2)$$

where τ is the photon optical depth. When the density is high, an atom which absorbs a photon will be collisionally deexcited before the photon can be reemitted, so P is just the probability that the photon will escape absorption. Since we see only one-third of the Fe, this suggests that $\tau \approx 3$.

Next we calculate the line optical depth by uniformly distributing all the Fe in the homologously expanding ejecta up to a velocity v. In the Sobolev approximation, the optical depth τ in a line in an expanding medium with a large velocity gradient at time t after the explosion is given by

$$\tau = (A_{ul}\lambda^3 g_u t/8\pi)(n_l/g_l - n_u/g_u), \quad (3)$$

where g_u (g_l) are the statistical weights of the upper (lower) states. An estimate of the density comes from derived mass and the constraint that the line-emitting region has $v \approx 2000$ km s^{-1}. Taking the mass of Fe II found above, this leads to τ([Fe II] 25.98) ≈ 0.51 and τ([Fe II] 19.93) ≈ 0.42. The level population has been calculated assuming LTE at 6000 K.

The assumption of uniform density leads us to conclude that the optical depth in the Fe II line is small, yet we see only a fraction of the Fe known to be present. This suggests that the Fe is distributed nonuniformly throughout the emitting volume. There are two main possibilities regarding how the "missing" iron is hidden. In the first case, all the iron is located in clumps so that the observed fraction represents only that which is within one optical depth of the clump surface, or iron that may be present in the interclump medium. In the second, most of the iron is centrally condensed with the remaining fraction (equal to $\approx$one-third) distributed uniformly throughout a much larger optically thin volume of the ejecta. If all the iron is in optically thick clumps (the first case), then the temperature previously calculated is incorrect. However, if we primarily observe the distributed, optically thin, iron component (second case), then the temperatures derived in the previous section pertain to the gas in this optically thin component, because the remaining optically thick component will contribute little to the total line flux. The two possibilities may be distinguished by following the temporal evolution of the Fe line shape and strength in the ejecta. If the clumps are uniformly distributed in the ejecta, the line shape will be unchanged as it increases in intensity. In the second case, as the centrally condensed iron becomes optically thin, most of the increase in the line will occur at low velocities, increasing the flux density near line center with respect to the wings.

Since the ionization potentials of Ni, Co, and Fe are essentially identical, the ionization states of Ni, Co, and Fe will therefore be very similar, so that most of the Co will be in the form of Co II. The mass implied for Co is $\approx 0.005\ M_\odot$ if all of the flux at 18.8 μm (after subtracting the H contribution) is due to [Co II]. The mass of Co is close to the $0.0073\ M_\odot$ expected from the radioactive decay of $0.075\ M_\odot$ of ^{56}Ni on day 268, implying that this component in the ejecta is optically thin. This fact essentially rules out the possibility of continuum absorption being the opacity source for the Fe lines.

c) *Contribution of Hydrogen Free-Free to the Continuum*

The strength of the H lines allows us to estimate what contribution to the observed free-free emission is due to ionized H.

The emissivity of H I 7-8 is (Hummer and Storey 1987)

$$\epsilon(7\text{-}8) = 0.45 \times 10^{-27} \times T_4^{-1.23} \text{ ergs cm}^{-3} \text{ s}^{-1} , \quad (4)$$

where T_4 is the temperature in 10^4 K. The luminosity in the line is

$$L(7\text{-}8) = \epsilon(7\text{-}8) n_e n_{\text{H II}} V , \quad (5)$$

so the product is equal to $(3.2 \pm 0.3) \times 10^{64} T_4^{-1.23}$ cm^{-3}. The fractional contribution of H I to the measured free-free excitation parameter is $(0.73 \pm 0.08) T_4^{-0.82}$. Unless the temperature is as high as 15,000 K, only a fraction (65% for $T = 6000$ K) of the free-free emission is due to H, and the rest of the emission must be due to ionized metals. If the temperature were 15,000 K, then the ionization state would be higher, and the spectrum would be dominated by Fe III instead of Fe II. It is likely that the non-H free-free emission is due to the ionized heavy elements which produce the far-infrared line emission and therefore arises from the same volume within the ejecta.

In the line-emitting region $\langle Z \rangle \sim 1$, therefore, $n_e \approx n_i$, and so

$$n_e^2 V(\text{line}) \approx 4.4 \times 10^{64} \times (1 - 0.73\ T_4^{-0.82}) , \quad (6)$$

where V(line) is the volume of the line-emitting region. From blackbody arguments, we show that the FWHM line width is greater than 1700 km s^{-1}. The slowest moving H is at 2200 km s^{-1} (Elias *et al.* 1988), and therefore most of the heavy elements in the line-emission region are probably expanding no faster than this and most likely have a velocity of about 2000 km s^{-1}. In this case, the electron density in the line-emission region is

$$n_e \approx 3.3 \times 10^8 \times (1 - 0.73 \times T_4^{-0.82})^{0.5} , \quad (7)$$

and the associated mass is $\approx 1.8 \langle A \rangle / 28 (1 - 0.73 T_4^{-0.82})^{0.5}$ $M_\odot$, where $\langle A \rangle$ is the mean atomic mass, here taken to be that of Si. The inferred electron densities are clearly very high.

IV. THE CONTINUUM EMISSION COMPONENT

A striking feature of the spectrum is the flat continuum, defined by the lower envelope of the emission spectrum, which extends from 16.6 to 65 μm in our observations. Together with the 50 and 100 μm photometric observations of Harvey, Lester, and Joy (1987), and the 4–13 μm observations of Rank *et al.* (1988), we find that the continuum is a quite flat function of wavelength in at least the 4–100 μm wavelength regime. The spectrum could be due to dust emission or synchrotron emission from newly accelerated electrons. However, the flatness of the spectrum and its observed decline on 1988 February 25 in the 8–13 μm observations of Aitken *et al.* (1988), and more consistent with the behavior of a free-free emission spectrum. Our observations, combined with the nondetection of SN 1987A by radio observers, put constraints on the physical conditions in the emitting region.

a) The Ionization and Energy Balance of the IR–emitting Region

The IR flux from an ionized gas at temperature T and distance D is given by

$$F_\nu(\text{Jy}) = 5.71 \times 10^{-59} \sum g_{\text{ff}} Z_i^2 n_e n_i V / [D_{\text{kpc}}^2 T^{1/2} \exp(h\nu/kT)] , \quad (8)$$

where n_e, n_i are, respectively, the electron and ion density in the ejecta. V is the volume (in cm^3) of the emitting region, D_{kpc} ($= 50$) is the distance to the supernova in kiloparsecs, and g_{ff} is the temperature-averaged Gaunt factor. The low-ionization state of the heavy elements suggests that $Z_i \approx 1$, giving $F_\nu(\text{Jy}) \approx 2.86 \times 10^{-64} n_e n_Z V T_4^{-1/2} \exp[-1.4388/\lambda\,(\mu\text{m})\, T_4]$, where T_4 is the gas temperature in units of 10^4 K, $g_{\text{ff}} \approx 1.25$, and n_Z is the density of all ionized heavy elements in the ejecta. Following Aller (1984), we define an "excitation parameter" ζ (units of cm^{-3}), given by

$$\zeta = \sum Z_i^2 n_e n_i V \approx n_e n_Z V . \quad (9)$$

The parameter ζ can be expressed in terms of the continuum free-free flux at frequency ν, F_ν, as

$$\zeta \approx 3.5 \times 10^{63} T_4^{1/2} \exp[1.4388/\lambda(\mu\text{m})T_4] \times F_\nu \text{ (Jy) cm}^{-3} . \quad (10)$$

For a 20 μm flux density of 10 Jy and $T_4 \approx 1$, we get $\zeta \approx 3.8 \times 10^{64} T_4^{1/2}$ cm^{-3}.

The recombination time, $t_{\text{rec(s)}}$, in the free-free emitting region is $(n_e \alpha_R)^{-1} \approx 3.8 \times 10^7\ T_4^{0.8}\ (10^5/n_e)$, where $\alpha_R \approx 2.6 \times 10^{-13} T_4^{-0.8}$ cm^3 s^{-1}, is the recombination coefficient to the $n = 2$ state of H-like ions (Osterbrock 1973). The recombination time $t_{\text{rec}}(\text{s}) \approx 3.8 \times 10^7\ T_4^{0.8} (10^5/n_e)$ will therefore be considerably shorter than the dynamical lifetime of the ejecta ($\sim$9 months), since densities in the emitting region are significantly higher than 10^5 cm^{-3} (see § IV below). We conclude that a continuous source of energy is required to maintain the ionization in the ejecta.

Figure 4 shows the observed flux from SN 1987A in the X-ray to FIR wavelength regime around 1987 November. The figure shows that most of the SN output appears at visual and near-IR wavelengths. The total flux given by the photometric

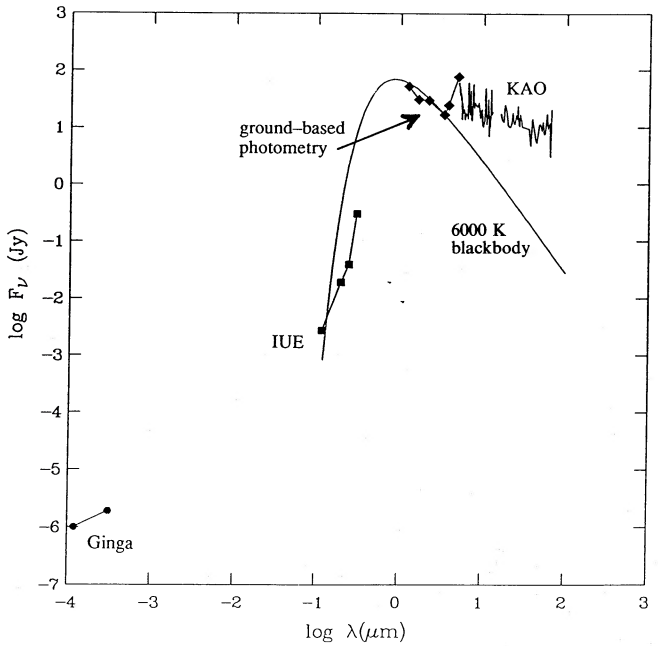

FIG. 4.—Observed flux from SN 1987A in the X-ray to FIR wavelength regime around 1987 November. Most of the SN output appears at visual and near-IR wavelengths. There is no evidence for thermal emission from dust in the spectrum of the supernova. The Ginga observations were taken from Dotani *et al.* (1987), *IUE* data were provided by Sonneborn (1987), infrared photometric data were taken from Whitelock *et al.* (1988), and the 5–10 μm IR observations were taken from Rank *et al.* (1988). Also shown is a 6000 K blackbody.

measurement on day 260 (Whitelock *et al.* 1988) is 3.7×10^{-14} W cm^{-2}, corresponding to a luminosity of 11.2×10^{40} ergs s^{-1} for an adopted distance of 50 kpc. This luminosity is approximately equal to the total radioactive decay energy emitted by the 0.075 $M_\odot$ of ^{56}Co widely believed to power the optical light curve of the supernova (e.g., Woosley 1988; Itoh *et al.* 1987). The optical light curve is dominated by line emission (e.g., Whitelock *et al.* 1988), suggesting that the ejecta entered a nebular emission phase. For comparison, the flux emitted in lines in the 20–70 μm regime is $\sim 2.6 \times 10^{-17}$ W cm^{-2}, whereas the IR continuum flux is 3×10^{-16} W cm^{-2}. Only $\sim 1\%$ of the total radioactive decay energy emanates, therefore, as free-free emission.

The UV visual luminosity required to maintain the ionization by direct photoionization is given by $\zeta \alpha_R P_i \approx 2 \times 10^{40} P_i$ (eV) ergs s^{-1}, where P_i is an average ionization potential. For $P_i \approx 10$ eV, typical of the elements in the mantle, the required UV luminosity is $\approx 2 \times 10^{41}$ ergs s^{-1}. This luminosity is larger than the total bolometric luminosity observed on day 266 by a factor of 2, and considerably larger than the available energy in ionizing (>10 eV) photons (see Fig. 4). This rules out direct photoionization as the mechanism for maintaining this mass of ionized gas.

Similarly, we can show that the ionization cannot be maintained by the fast electrons produced by Comptonization of the γ-rays, as is the case for type I supernovae (Meyerott 1980; Axelrod 1980). The ionization rate due to fast electrons can be written as S/W_i, where S is the total energy deposition rate (ergs s^{-1}) in the ejecta and W_i is the work per ion pair. Balancing the recombination rate requires an energy input rate $S \approx W_i(n_e n_Z \alpha_R V) = \zeta \alpha_R W_i$. In supernova ejecta, the value of W_i is about $30P_i$, significantly higher than the value of $\approx 2P_i$ observed in gases, since secondary electrons thermalize with the free electron gas before causing further ionization (Axelrod 1980). For $P_i = 10$ eV and $\zeta \approx 4 \times 10^{64}$ cm^{-3}, as implied by our continuum observations, the required energy deposition rate is $S \approx 6 \times 10^{42}$ ergs s^{-1}. This value exceeds the available radioactive decay energy available on day 266 by a factor of ~ 50. This problem is a general one in type II supernovae, in which the H recombination time is shorter than the age of the envelope (Kirshner and Kwan 1974, 1975). To explain the observed optical emission, Kirshner and Kwan invoked ionization from the $N = 2$ state as a mechanism for replenishing the electron population in the ejecta.

These difficulties lead us to consider the possibility that the ionization in SN 1987A is maintained by ionization from excited electronic states by thermal electrons or photons. The ionization must proceed from excited electronic states with low ionization potentials ($\approx$few eV) to satisfy the energy constraint $2 \times 10^{40} P_i$ (eV) $< 1.1 \times 10^{41}$ ergs s^{-1}. The same conclusion was reached by Aitken *et al.* (1988) in their analysis of the origin of the free-free emission from the supernova. Also, Xu and McCray (1988) suggested that the ionization is predominantly maintained by photoionization from excited atomic levels, since most of the energy of the primary electrons is channeled toward the production of ionizing photons. The general situation is very similar to that encountered in quasars (e.g., Collin-Souffrin *et al.* 1980; Davidson and Netzer 1979), where Lyα trapping maintains a fraction of the H atoms in their excited state, greatly enhancing the ionization rate of the gas. This requires continuous replenishment of the population of ionizing photons or electrons. The population of ionizing electrons is maintained by the slowing down of the primary fast electrons. Typical slowing-down times are $\approx 2 \times 10^6/n_e$ days (Axelrod 1980), significantly shorter than the expansion time of the ejecta for densities above $\sim 10^6$ cm^{-3} (see below).

b) *The Dimension and Physical Conditions of the Emitting Region*

The size of the continuum emission region can be estimated from the fact that it is still marginally thin at about 50 μm. For a given value of ζ, the condition that $\tau_{\rm ff} = \alpha_{\rm ff} R \approx 1$, is equivalent to the requirement that $R^2 \approx 3\alpha_{\rm ff} V/4\pi$, where

$$\alpha_{\rm ff}\ ({\rm cm}^{-1}) = 2.0 \times 10^{-31}\ \lambda\ (\mu{\rm m})^2 \sum g_{\rm ff} Z_i^2 n_e n_i T^{-3/2} \quad (11)$$

is the free-free absorption coefficient in the Rayleigh-Jeans regime (e.g., Rybicki and Lightman 1979, p. 160). For $T = 6000$ K, we find that the resulting lower limit on the size of the free-free emitting region is $R \approx 4 \times 10^{15}$ cm, which corresponds to an expansion velocity of ~ 1700 km s^{-1}. This velocity is lower than the lowest observed hydrogen velocities in the Bracket-Paschen lines which are approximately 2100 km s^{-1} (see discussion in Woosley 1988), consistent with a picture in which both the hydrogen and heavy elements contribute to the free-free emission. From the size of the emitting volume and the fact that $\zeta \approx 4 \times 10^{64}$ cm^{-3}, we calculate an average electron density of $\approx 4 \times 10^8$ cm^{-3} and a total number of $\sim 10^{56}$ electrons in the free-free emitting region. If 35% of the free-free emission originates from the metal-rich ejecta, which has a total number of $\approx 1.5 \times 10^{56}$ nuclei heavier than He, then the observations imply a metallic ionization fraction of $\sim 30\%$ in the mantle.

c) *Limits on Circumstellar Dust*

Two separate observations suggest that dust may be present around SN 1987A. Ultraviolet (UV) observations of the SN revealed the presence of narrow emission lines of various ionized species with line widths less than ~ 30 km s^{-1} (Fransson *et al.* 1989). The low line velocities suggest that they originate from a circumstellar shell, lost by the progenitor star during the red supergiant phase of its evolution and excited by the initial (unobserved) EUV burst of the supernova. If dust formed during the red giant mass loss phase, then it could give rise to an observable IR echo (Chevalier 1987; Dwek 1988*b*). Infrared echoes may also arise from dust closer to the SN (distance of ~ 3 light-months), the presence of which was suggested by infrared speckle observations of the SN (Chalabaev, Perrier, and Mariotti 1989). The absence of any evidence for far-infrared emission from dust can be used to put upper limits on the mass of the circumstellar shell. For an upper limit of 10 Jy the upper limit on the shell mass is $\sim 10(Z_d/0.00025)^{-1} M_\odot$, where Z_d is the dust to gas mass ratio in the shell (Dwek 1988*c*). This upper limit is too large to provide any useful constraints on the evolution of the progenitor star.

V. CONCLUSIONS

Our far-infrared observations have provided a look deep inside SN 1987A about 270 days after the explosion. These observations provided a first "unbiased" look at the composition and physical condition of the emitting region. Most of the infrared energy is emitted in a flat continuum that extends over the entire spectral range (16–66 μm) of our observations. This continuum is best explained as free-free emission from regions of ionized hydrogen in the inner envelope and regions of ionized heavy elements in the mantle. From the strength of the hydrogen lines, we can estimate the contribution of H^+ to the

free-free continuum. We find that at $T = 6000$ K, the H contribution is $\sim 65\%$, with the heavy elements in the mantle contributing the remaining emission.

We found that it is energetically impossible to maintain the requisite ionization level in the ejecta by ionizing the various elements, either by direct photoionization or by nonthermal electrons, from their ground state. Their ionization must therefore proceed from excited electronic states near the ionization limit. The population of excited states can be maintained by absorption of trapped resonance-line radiation. The atoms are then ionized from these excited states either by collisions with thermal electrons or by photons.

Lines of different ionization states and excitation levels of some elements fall in our spectral range, and the presence (or absence) and relative strength of these lines provide us with an excellent picture of the ionization state and electron temperature in the metal-rich ejecta. We find that Fe is almost all singly ionized, and that the electron temperature is 6000^{+2000}_{-1000} K.

The absolute line strengths can be used to estimate the total mass of various heavy elements. The inferred masses of these elements are much larger than those expected to be present in the progenitor star prior to the SN event, implying that the elements are the products of explosive nucleosynthesis. The inferred Fe mass is 0.021 $M_\odot$, which is less than the 0.065 $M_\odot$ expected at day 266 from the radioactive decay of ^{56}Co. This implies that the Fe lines are optically thick. From simple blackbody arguments, we can see that the implied FWHM expansion velocity is greater than 2000 km s^{-1}. If the 0.065 of Fe were spread uniformly over this volume, the lines would be optically thin. The fact that we see only one-third of the Fe in the ejecta suggests that the iron is either in optically thick clumps or centrally condensed in an optically thick, slow-moving volume.

All the observed infrared emission can be explained as either free-free or line emission from the expanding ejecta. We see no evidence, therefore, for thermal emission from dust either in the expanding ejecta or in the circumstellar shell around the supernova.

We expect the free-free emission to drop sharply as the density and ionization decrease in the ejecta. The strength of the hydrogen lines should decrease correspondingly. In contrast, we expect the Fe lines to increase in strength as the ejecta become more optically thin. The relative strength of the excited state lines should decrease with decreasing mantle temperature. Continued observations in this spectral range should provide increasingly accurate estimate of the masses of the heavy elements, temperature, and ionization state of the supernova mantle.

We thank the staff of the KAO for its excellent support during the observations. We thank Brent Mott for constructing the detector array used for these observations, Clell Scearce, Crockett Lowe, Carrol Sappington, and Dave Dargo for their help in the preparation of the instrument, and Ken Stewart and Jim Heaney for their assistance in calibrating the instrument. We also acknowledge helpful scientific discussions with David Aitken, Dick McCray, and Stan Woosley. This work was supported by the NASA Airborne Astronomy Program.

REFERENCES

Aitken, D. K., Smith, C. H., James, S. D., Roche, P. F., Hyland, A. R., and McGregor, P. J. 1988, *M.N.R.A.S.*, **235**, 19.
Aller, L. H. 1984, *Physics of Thermal Gaseous Nebulae* (Dordrecht: Reidel).
Axelrod, T. S. 1980, Ph.D. thesis, University of California.
Brocklehurst, M. 1970, *M.N.R.A.S.*, **148**, 417.
———. 1971, *M.N.R.A.S.*, **153**, 471.
Chalabaev, A. A., Perrier, C., and Mariotti, J. M. 1989, *Astr. Ap.*, **210**, L1.
Chevalier, R. A., and Kirshner, R. P. 1979, *Ap. J.*, **233**, 154.
Clayton, D. D. 1982, *Quart. J.R.A.S.*, **23**, 174.
Colgan, S. W. J., and Hollenbach, D. 1988, *Ap. J. (Letters)*, **329**, L25.
Collin-Souffrin, S., Dumont, S., Heidmann, N., and Joly, M. 1980, *Astr. Ap.*, **83**, 190.
Conrath, B. J. 1986, private communication.
Davidson, K., and Netzer, H. 1979, *Rev. Mod. Phys.*, **51**, 715.
Dotani, T., *et al.* 1987, *Nature*, **330**, 230.
Dwek, E. 1988*a*, *Ap. J.*, **329**, 814.
———. 1988*b*, in *Supernova 1987A in the Large Magellanic Clouds*, ed. M. Kafatos and A. G. Michalitsianos (Cambridge: Cambridge University Press), p. 240.
———. 1988*c*, *Proc. Astr. Soc. Australia*, **7**, 468.
Elias, J. H., Gregory, B., Phillips, M. M., Williams, R. E., Graham, J. R., Meikle, W. P. S., Schwartz, R. D., and Wilking, B. 1988, *Ap. J. (Letters)*, **331**, L9.
Fransson, C., Cassatella, A., Gilmozzi, R., Kirshner, R. P., Panagia, N., Sonneborn, G., and Wamsteker, W. 1989, *Ap. J.*, **336**, 429.
Fransson, C., and Chevalier, R. A. 1987, *Ap. J. (Letters)*, **322**, L15.
Gehrz, R. D., and Ney, E. P. 1987, *Proc. Nat. Acad. Sci.*, **84**, 6961.
Glaccum, W. 1989, Ph.D. thesis, in preparation.
Graham, J. R., Meikle, W. P. S., Allen, D. A., Longmore, A. J., and Williams, P. M. 1986, *M.N.R.A.S.*, **218**, 93.
Graham, J. R., Wright, G. S., and Longmore, A. J. 1987, *Ap. J.*, **313**, 847.
Hanel, R., *et al.* 1986, *Science*, **233**, 70.
Harvey, P. M., Lester, D., and Joy, M. 1987, *IAU Circ.*, No. 4518.
Hummer, D. G., and Storey, P. J. 1987, *M.N.R.A.S.*, **224**, 801.
Itoh, H. 1987, *Pub. Astr. Soc. Japan*, **40**, 263.
Itoh, M., Kumagai, S., Shigeyama, T., Nomoto, K., and Nishimura, J. 1987, *Nature*, **330**, 233.
Kirshner, R. P. 1988, in *Supernova 1987A in the Large Magellanic Cloud*, ed. M. Kafatos and A. G. Michalitsianos (Cambridge: Cambridge University Press), p. 87.
Kirshner, R. P., and Kwan, J. 1974, *Ap. J.*, **193**, 27.
———. 1975, *Ap. J.*, **197**, 415.
Kozasa, T., Hasegawa, H., and Nomoto, K. 1989, *Ap. J.*, **344**, 325.
Mendoza, C. 1983, in *IAU Symposium 103, Planetary Nebulae*, ed. D. R. Flower (Dordrecht: Reidel), p. 143.
Meyerott, R. E. 1980, *Ap. J.*, **239**, 257.
Nussbaumer, H., and Storey, P. J. 1982, *Astr. Ap.*, **110**, 295.
———. 1988*a*, *Astr. Ap.*, **193**, 327.
———. 1988*b*, *Astr. Ap.*, **200**, L25.
Odenwald, S. 1983, private communication.
Osterbrock, D. E. 1973, *Astrophysics of Gaseous Nebulae* (San Francisco: Freeman).
Phillips, M. N., Heathcote, S. R., Haumy, M., and Navarrete, M. 1988, *A.J.*, **95**, 1087.
Rank, D. M., Pinto, P. A., Woosley, S. E., Bregman, J. D., Witteborn, F. C., Axelrod, T. S., and Cohen, M. 1988, *Nature*, **331**, 505.
Rybicki, G. B., and Lightman, A. P. 1979, *Radiative Processes in Astrophysics* (New York: Wiley).
Sonneborn, G. 1987, private communication.
Spencer, J. R. 1987, Ph.D. thesis, University of Arizona.
Whitelock, P. A., *et al.* 1988, *M.N.R.A.S.*, **234**, 5.
Wiese, W. L., Smith, M. W., and Glennon, B. M. 1966, *Atomic Transition Probabilities*, Vol. **1**, (NSRDS-NBS 4).
Wiese, W. L., Smith, M. W., and Miles, B. M. 1969, *Atomic Transition Probabilities*, Vol. **2** (NSRDS-NBS 22).
Winkler, P. F., and Kirshner, R. P. 1985, *Ap. J.*, **299**, 981.
Witteborn, F., Bregman, J., and Wooden, D. 1988, *IAU Circ.*, No. 4592.
Woosley, S. E. 1988, *Ap. J.*, **330**, 218.
Woosley, S. E., Pinto, P. A., and Ensman, L. 1988, *Ap. J.*, **324**, 466.
Wright, E. L. 1976, *Ap. J.*, **210**, 250.
Xu, Y., and McGray, R. 1988, *Bull. AAS*, **20**, 959.

E. Dwek, S. H. Moseley, and R. F. Silverberg: Code 685, NASA Goddard Space Flight Center, Greenbelt, MD 20771

W. Glaccum: Code 4138GL, Naval Research Laboratory, Washington, DC 20375-5000

J. R. Graham: Downs Laboratory, California Institute of Technology 320-47, Pasadena, CA 91125

R. F. Loewenstein: Yerkes Observatory, Williams Bay, WI 53191